frontiers | Frontiers in Materials

TYPE Original Research
PUBLISHED 23 February 2024
DOI 10.3389/fmats.2024.1358912

OPEN ACCESS

EDITED BY
Giuseppe Failla,
Mediterranea University of Reggio Calabria, Italy

REVIEWED BY
Kaushal Kishore,
Tata Steel, India
Zhixian Peng,
Wuhan University of Science and Technology, China

*CORRESPONDENCE
Shuchao Zhang,
zhangshuchao@jsit.edu.cn
Jinliang Du,
jinliangdo@163.com

RECEIVED 20 December 2023
ACCEPTED 29 January 2024
PUBLISHED 23 February 2024

CITATION
Yu Y, Wang Z, Chen B, Zhang S and Du J (2024), Impact of various heat treatment processes and welding speeds on the mechanical properties and microstructures of soft/hard composite joints.
Front. Mater. 11:1358912.
doi: 10.3389/fmats.2024.1358912

Impact of various heat treatment processes and welding speeds on the mechanical properties and microstructures of soft/hard composite joints

Yang Yu[1], Zhao Wang[2], Biao Chen[1], Shuchao Zhang[3]* and Jinliang Du[4]*

[1]Shougang Group, Shougang Jingtang United Iron and Steel Co., Ltd., Tangshan, China, [2]Tangshan Iron and Steel Group Co., Ltd., Tangshan, China, [3]School of Microelectronics, Jiangsu Vocational College of Information Technology, Wuxi, China, [4]College of Metallurgy and Energy, North China University of Science and Technology, Tangshan, China

There is a certain contradiction between the formability and strength of auto parts. In this work, the whole-process processing technology of hot stamping soft steel was designed, and 500 MPa grade mild steel (500HS) with uniform microstructure was prepared. To take into account the strength and formability of hot stamping soft steel, here, based on laser welding technology, 500 MPa grade soft steel, and 1500 MPa grade hard steel are benignly composited, and by adjusting the laser welding speed and heat treatment process, the loss of mechanical properties caused by the weld seam is eliminated. A soft/hard composite steel for automobiles with excellent strength, ductility and formability is obtained. To maintain excellent deformation resistance and bonding force of the weld, the heat-affected zone of 500HS retains part of bainite and pearlite, which is beneficial to the strain compatibility and stress partitioning with the microstructure of the base metal, and the hardness is low. After heat treatment, which helps to transfer the stress concentration effect to the 500HS base metal with strong energy absorption capacity, so that the clad steel has excellent comprehensive mechanical properties. This process is developed based on existing industrialized equipment and has broad application prospects.

KEYWORDS

hot stamping steel, full process design, automotive steel, laser welding, mechanical property

1 Introduction

Lightweight is the main measure to achieve energy saving and emission reduction in the automotive industry in the future, and the use of advanced high-strength steel (AHSS) is an effective way to ensure vehicle safety performance and lightweight (Li et al., 2019; Du et al., 2021; Dong et al., 2022; Hong et al., 2022; Lai et al., 2022). AHSS is usually composed of two-phase or multi-phase microstructures with huge differences in mechanical properties (Sun et al., 2018; Feistle et al., 2022; Sedaghat-Nejad et al., 2022). The high tensile strength of AHSS is at the cost of reduced plasticity, which leads to intergranular stress concentration during the stamping forming

TABLE 1 Composition of experimental steel.

Materials	C	Mn	S	P	Si	Al	Nb	Ti	Cr
T1500HS	0.222	1.31	0.002	0.014	0.26	0.04	-	0.046	0.23
500HS	0.07	1.55	0.002	0.012	0.02	0.04	0.045	0.070	-

FIGURE 1
Preparation process of soft/hard composite forming steel.

process, causing cracking and wrinkling of the material, which limits the application of AHSS in the body (Soleimani et al., 2020; Costa et al., 2022; Zhang and Xu, 2022).

To solve the contradiction between the high strength and formability of materials (Hu et al., 2017; Cann et al., 2021; Razmpoosh et al., 2021), Zhang et al. (2023) increased the diffusion ability of atoms and enhanced the migration ability of grain boundaries through high temperature, combining stamping forming with heat treatment effectively, ultra-high-strength hot stamping steels are obtained. The ultra-high strength of hot-formed steel is caused by a high content of martensite, and ferrite or bainite is used to coordinate the plasticity of hot-formed steel. Process parameters such as austenitizing temperature, holding time, initial deformation temperature, and cooling rate have a significant impact on the microstructure and mechanical properties of hot-stamped steel (Zhao et al., 2022). Zhao et al. (2022) introduced a full martensitic structure into 38MnB5 through a cooling rate greater than 30K/s, so that the strength reached 2 GPa, but the

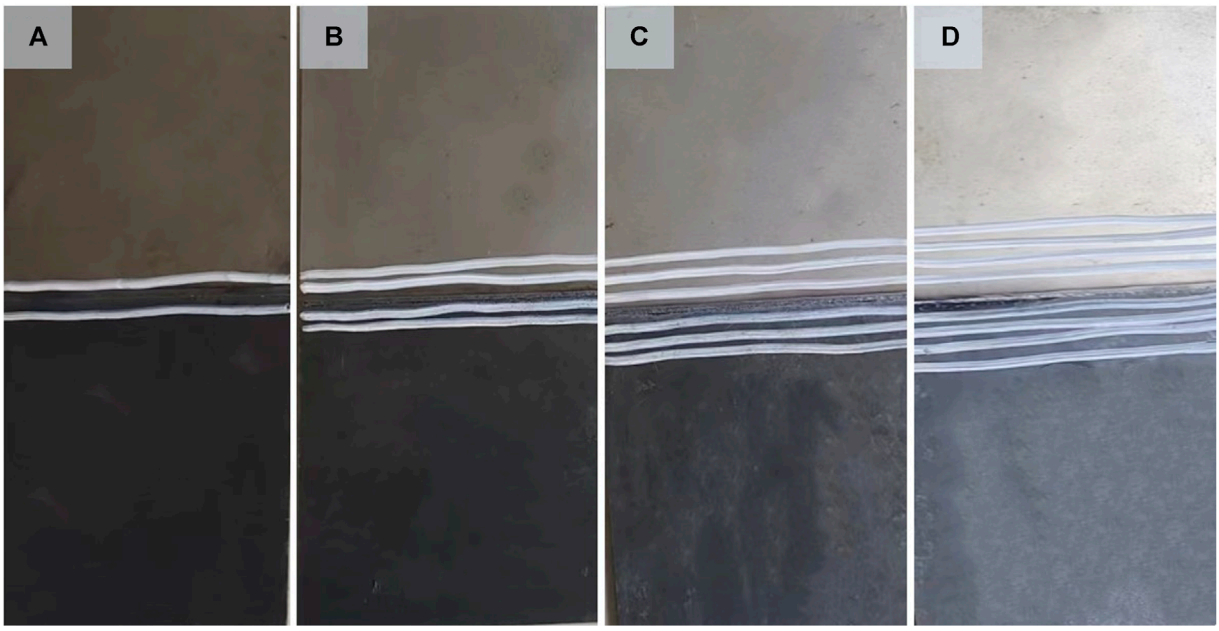

FIGURE 2
Macroscopic morphology of T1500HS and 500HS after laser welding, **(A)** V1, **(B)** V2, **(C)** V3, **(D)** V4. The welding joints are marked with different numbers of white lines, corresponding to V1, V2, V3, and V4, respectively.

plasticity was poor. Since several thin martensite strips with different orientations can be formed in a single prior austenite grain and arranged in parallel, there is often a large orientation difference between these strips, which makes it have poor impact resistance. (Dong et al., 2022; Zhang et al., 2023). Manladan et al. (2023) found that compared with the complete martensitic structure, retaining a small amount of ferrite or bainite reduces the strength of the steel, but it can improve the plasticity and energy absorption capacity. Zhang et al. (2015) controlled the heating rate, holding time, and rapid quenching to make the tensile strength exceed 1,500 MPa while maintaining an elongation of 8%. At present, the strength of the widely used hot-formed steel is generally ~1,500 MPa, but the plasticity is still poor (Feistle et al., 2022; Manladan et al., 2023).

Although the forming and strength problems of a single part have been solved to a certain extent (Bhargava et al., 2018; Liang et al., 2021), in order to realize the overall design of a lightweight body, each part needs to meet different thicknesses and performance requirements. If the materials of all parts have the same grade, thickness, and performance, some parts will have a large performance margin and processing difficulty, and the cost will be high (Drexler et al., 2021). In addition, although the strength of hot-formed steel is high, its impact toughness is obviously insufficient (Feistle et al., 2022). Xu et al. (2023) proposed a soft/hard composite automotive structural material design method, using high-strength hot-formed steel as a whole, partially softening lower-strength hot-formed steel, and taking into account the overall impact energy absorption capacity of the body structure. For example, the upper part of the B-pillar is a crash support unit, and the lower part is a shock-absorbing unit. In order to realize the soft/hard composite structure of automotive parts, Yu et al. (2021) used local heat treatment of the thermoforming mold, so that the local soft area required by the part was cooled or tempered at a lower rate. This technology has poor precision in controlling the strength of the local soft area of the part, and the production efficiency is low. The laser tailor welding method can tailor and weld soft materials and ultra-high-strength materials together, and perform hot stamping at the same time to meet the requirements of different regions and different strengths of parts. Chen et al. (2022) found that when welding dual-phase steel and pure titanium, materials with a large difference in strength and hardness have differences in weldability. In addition, The temperature of the base metal is often low and the cooling rate of the weld is difficult to control, which often introduces uneven distribution of martensite and ferrite, and the quality of the weld is difficult to control. Šebestová et al. (2018) reduced the cooling rate of the weld by properly preheating the base metal, eliminated the coarse ferrite zone in the martensite structure, and improved the quality of the weld. However, this method consumes too much energy during the industrialization process. It has important scientific significance and industrial value to carry out the whole process of processing of soft/hard composite hot-forming steel.

Welding technology is commonly used in automobile manufacturing, and the most widely used technique is traditional spot welding, where two or more metal components are placed together and then welded by passing electric current through the contact point. This technique is typically applicable only to metals with good electrical conductivity, with limited adaptability, controllability, and automation. Laser welding, on the other hand, involves focusing a laser beam onto the welding joint and using the

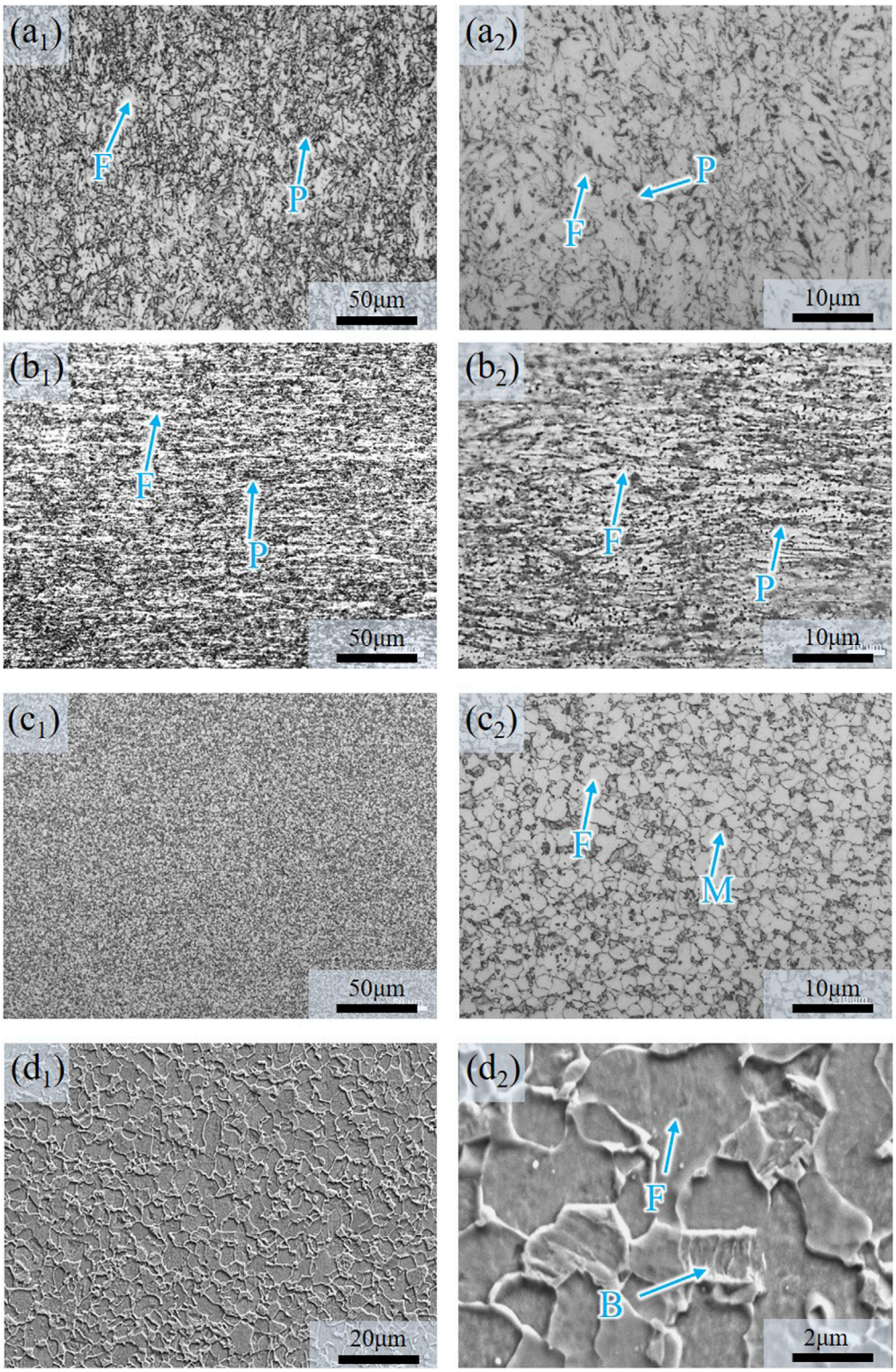

FIGURE 3
Microstructure during the preparation process of hot pressing-formed soft steel. **(a1–a2)** Microstructure observed by optical microscope (OM) after hot rolling of the sample. **(b1–b2)** Microstructure observed by OM after cold rolling and annealing of the sample. **(c1–c2)** Microstructure observed by OM after flat die quenching of the sample. **(d1–d2)** Microstructure observed by SEM after flat die quenching of the sample.

energy of the light to heat the joint to its melting point. Laser welding is often faster than traditional spot welding. The high energy density and adjustable focal length of the laser beam enable faster formation of weld seams, thereby increasing production efficiency. Traditional spot welding usually generates a relatively large heat-affected zone in the welding area, which may result in localized deformation

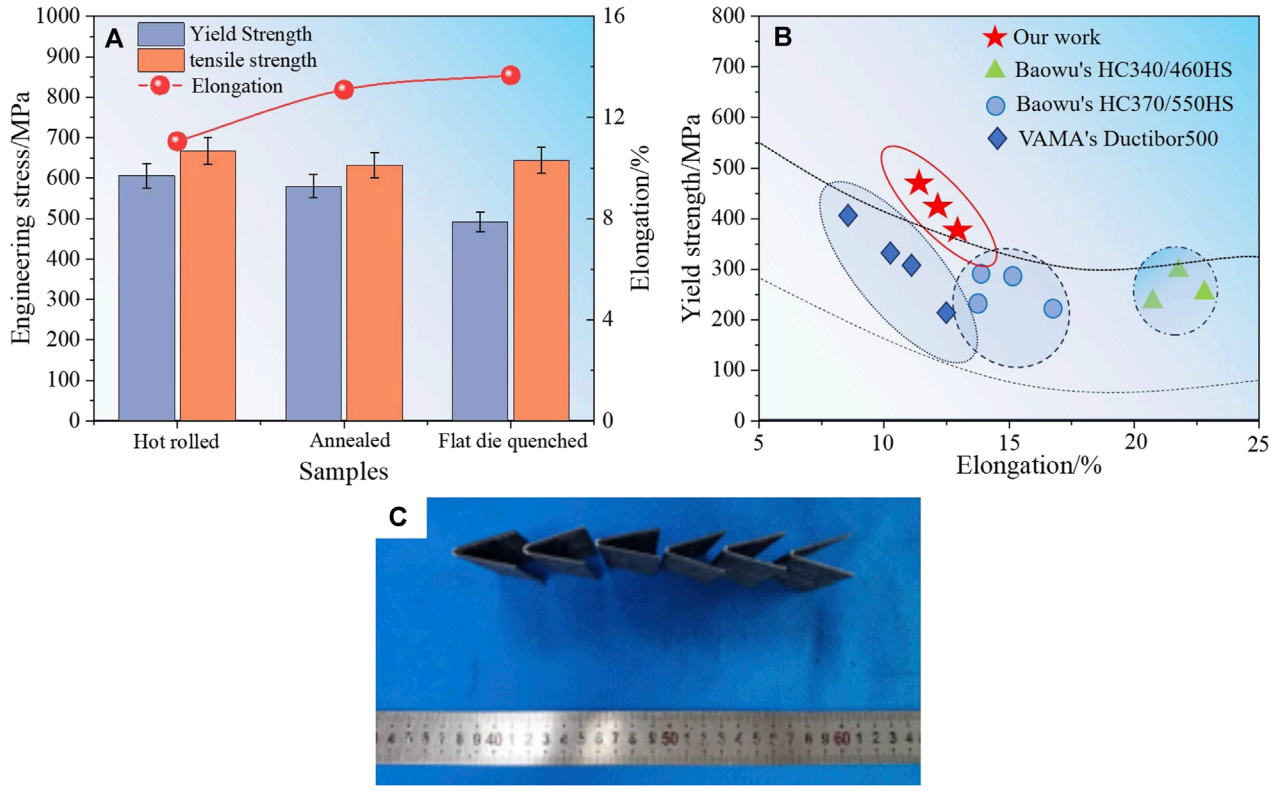

FIGURE 4
Mechanical properties of 500HS formed by hot stamping, **(A)** engineering stress-strain, **(B)** distribution diagram of yield strength and elongation, **(C)** bending test.

and decreased material performance. Laser welding has a smaller heat-affected zone, minimizing material deformation and thermal effects. It is also easier to integrate laser welding systems with robots or automatic conveyors, enabling highly automated welding processes and improving production efficiency and consistency. Therefore, developing composite technologies of automotive steels based on laser welding techniques holds significant application significance.

In this work, the whole-process preparation process of hot stamping forming steel with a yield strength of ~500 MPa is designed. Optimizing laser tailor welding parameters to design a soft/hard composite impact-resistant automotive steel with excellent energy absorption properties provides a theoretical and experimental basis for the development of automotive hot stamping steel.

2 Material and methods

In this work, steelmaking test with the composition shown in Table 1 was completed by using a multifunctional induction furnace. The billet is processed in the whole process as shown in Figure 1. After the billet is heated, dephosphorized, hot-rolled, layer cooling water, curled, sand blasted, cold-rolled, annealed, cooled, and flat-die quenched, it is laser-treated with ultra-high-strength steel Tailor welding and Erichsen cupping test.

2.1 Rolling and heat treatment

The slab whose composition is shown in Table 1 was heated to 1,220°C by 16166 CAL heating furnace, and the hot rolling experiment was started on a φ750 × 550 mm hot rolling mill. The final rolling temperature is 880°C, the crimping temperature is 650°C, and the final thickness of the hot-rolled sample is 3.0 mm. After the hot-rolled samples were sand-blasted to remove surface oxides, the cold-rolling test was completed on a φ450 mm straight-pull cold-rolling mill. Set the reduction rate to 53.33%, and the final thickness is 1.4 mm. The cold-rolled samples were annealed as shown in Figure 1. The cold-rolled sample was heated to 250°C at a heating rate of 6.94°C/s, then adjusted to 2.89°C/s and heated to 600°C. Subsequently, the heating rate was reduced again to 1.96°C/s, and after the sample reached 820°C, the heat preservation treatment was carried out for 89s. After completing the entire heating process, the sample was cooled to 700°C at a rate of 13.04°C/s. After holding at 700°C for 4s, it enters the fast cooling section. The rapid cooling section cools down to 360°C at a rate of 51.52°C/s. In the slow cooling section, the sample is overaged to 340°C at a cooling rate of 0.05°C/s and then cooled to 150°C at a cooling rate of 2.84°C/s. Finally quenched to room temperature. Samples are labeled 500HS.

The flat die quenching experiment was carried out using a 100t hydraulic press that can provide a pressure of 20MPa, and the temperature control accuracy was 1°C/s. The mold size is 400 ×

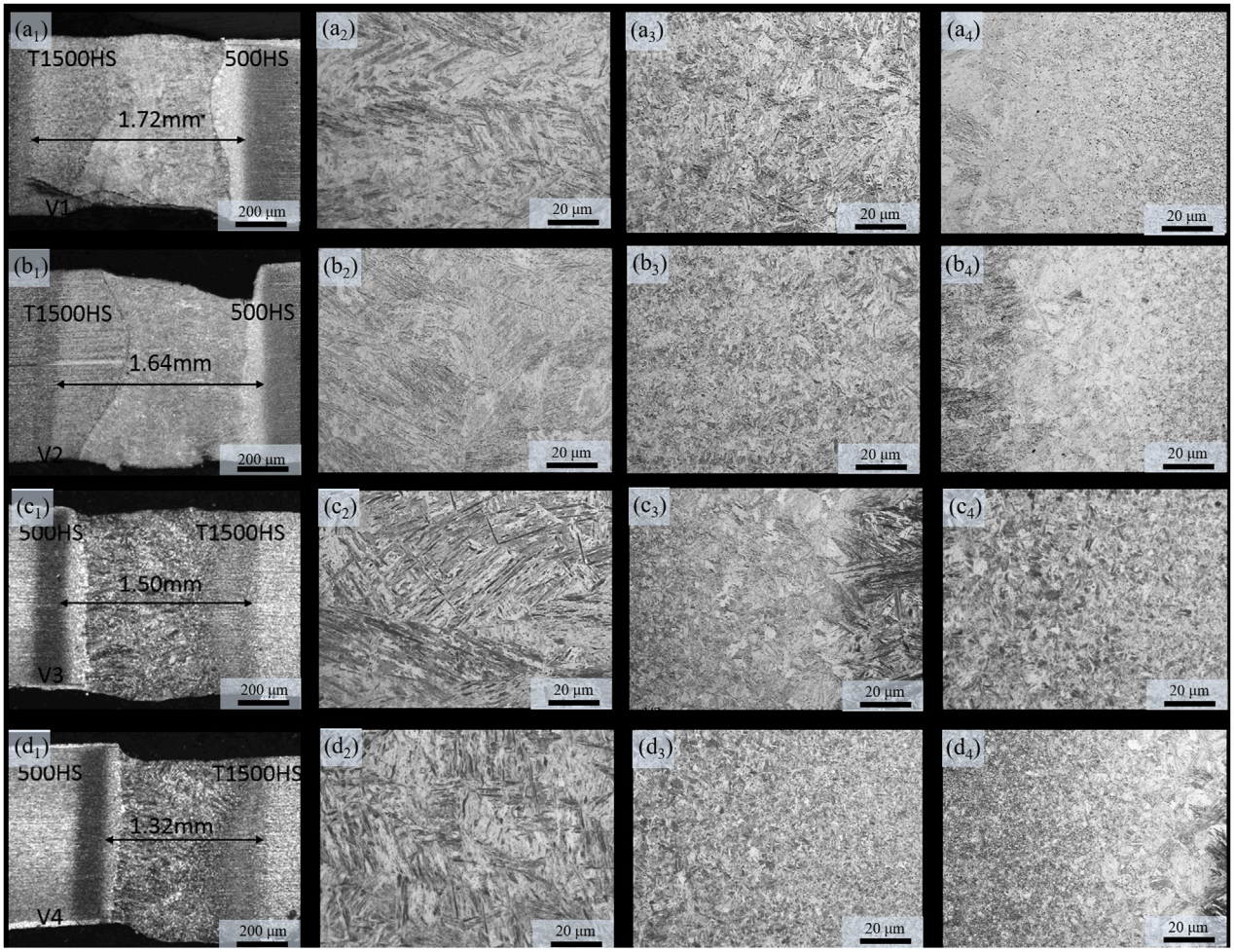

FIGURE 5
Microstructure of soft/hard composite steels, **(A_1~A_4)** V1, **(B_1–B_4)** V2, **(C_1–C_4)** V3, **(D_1–D_4)** V4.

400 mm, and the effective area is 320 × 320 mm. The lower mold is divided into left and right parts, which can be disassembled. The material of the mold is X153CrMoV12 tool steel. The cooling copper plate is connected to circulating water, and the cooling rate can reach ≥50°C/s.

2.2 Laser tailor welding

The basis for maintaining a constant laser power and changing laser speed is the thermal effect of the laser in the material processing. During the laser processing, controlling the laser power can affect the degree of melting and evaporation of the material, while changing the laser speed affects the interaction time between the laser and the material. Maintaining a constant laser power and increasing the laser speed will reduce the interaction time between the laser and the material, resulting in a decrease in the degree of melting and evaporation. This is applicable for finer welding and precise cutting. Conversely, reducing the laser speed increases the interaction time between the laser and the material, resulting in an increase in the degree of melting and evaporation. This is suitable for deeper cutting or welding requirements.

Therefore, based on the process requirements and desired processing effects, the laser speed can be adjusted to control the interaction time between the laser and the material to achieve the desired processing effect. At the same time, maintaining a constant laser power ensures the stability of the laser irradiation intensity, further affecting the uniformity and consistency of the processing quality.

T1500HS steel is a commercial advanced automotive steel provided by Tangshan Iron and Steel Group. Firstly, the 1.4 mm thick T1500HS and the 1.4 mm thick 500HS were cut into samples with a size of 100 × 100 mm through EDM. Laser tailor welding is performed using the laser tailor welding machine (SLCWF-X0610) shown in Figure 1. The welding parameters are: laser power is 2.0KW, welding speed is 2.5 m/min, 3 m/min, 3.5 m/min, 4 m/min, shielding gas flow rate is 20L/min, the samples of the four processes are named V1, V2, V3, and V4. Three sets of spare samples were welded by each process, and the hot stamping test was simulated after welding. Due to the small size of the samples, the plan was

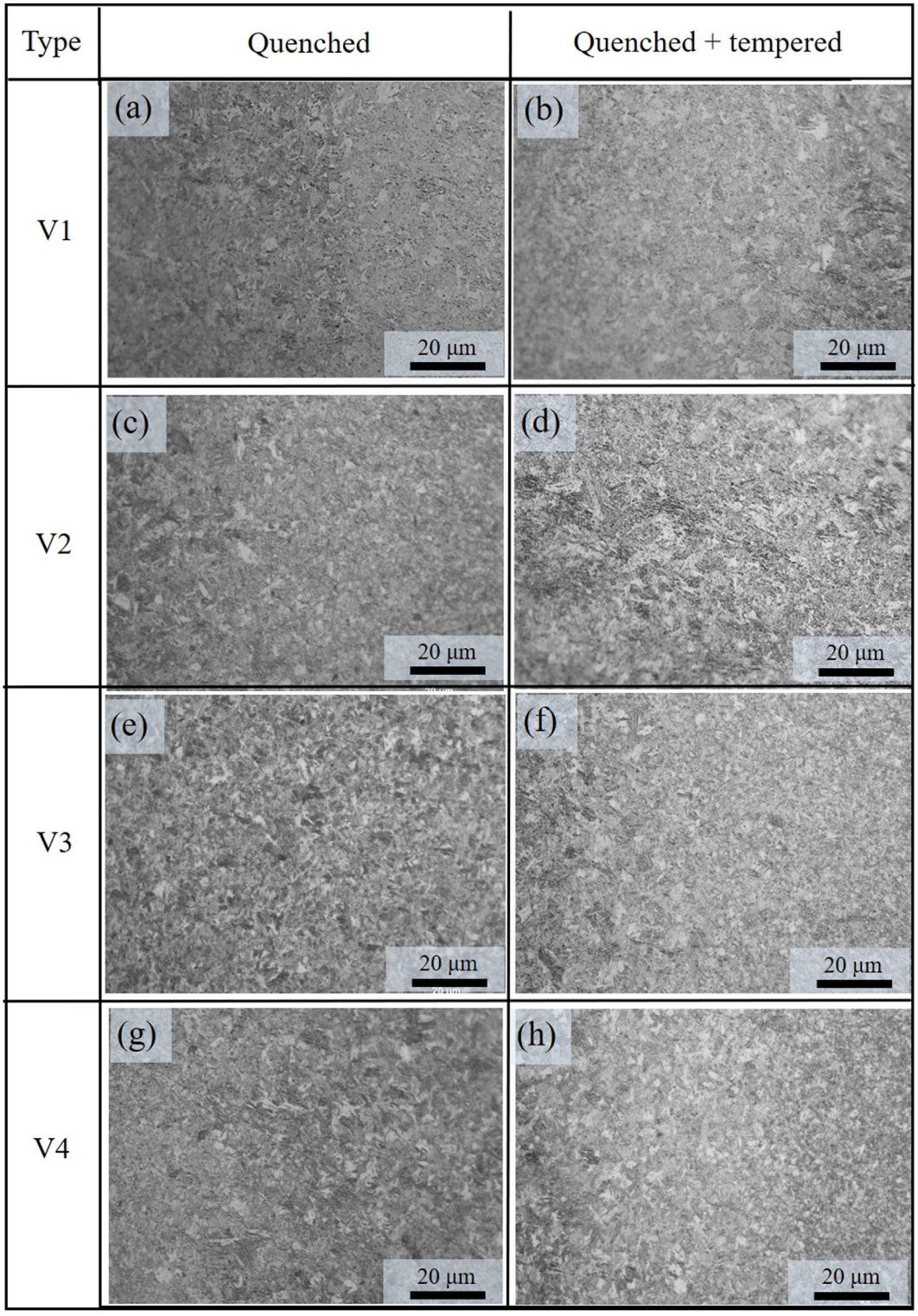

FIGURE 6
Microstructure of welds after heat treatment, **(A~D)** are quenched V1, V2, V3 and V4, **(E~H)** are quenched and tempered V1, V2, V3 and V4, respectively.

to place the tailored welded blank in a muffle furnace at 930°C, keep it warm for 5 min, and quickly move it to water for water quenching. Then take a group of quenched samples to simulate the paint baking process, put them in a furnace at 170°C for 20 min, and then cool them naturally. There are no defects on the front and back of the tailored welded blank, and there is no protrusion on the bottom, which meets the experimental requirements, as shown in Figure 2.

TABLE 2 Mechanical properties of welded joints.

Samples	Yield strength/Mpa	Tensile strength/Mpa	Elongation/%	Strength-plasticity product/Gpa	Fracture location
500HS annealing	510	572	14.6	8.35	-
500HS quenching	397	554	12.53	6.94	-
T1500HS annealing	431	638	25.5	16.27	-
T1500HS quenching	1,180	1,520	6.2	9.42	-
V1 annealing	499	694	8.49	5.89	500HS
V2 annealing	460	657	11.13	7.31	T1500HS
V3 annealing	464	647	11.57	7.49	500HS
V4 annealing	459	634	10.08	6.39	500HS
V1 quenching	899	1,065	3.68	3.92	500HS
V2 quenching	863	1,009	1.57	1.58	500HS
V3 quenching	938	1,064	3.44	3.66	500HS
V4-quenching	942	968	0.81	0.78	500HS
V1-temper	866	934	1.53	1.43	500HS
V2-temper	792	904	1.82	1.65	500HS
V3-temper	688	855	7.42	6.34	500HS
V4-temper	714	876	4.06	3.56	500HS

2.3 Microstructure and mechanical properties testing

After the metallographic sample is ground and polished, the surface is etched with 4% nitric acid alcohol solution for 2~4s, and then the macroscopic morphology and fine structure of the test sample are observed with a Zeiss optical microscope and a Zeiss scanning electron microscope.

Cutting from the middle of the sample into a dog-bone tensile sample with a width of 12.5 mm and a length of 70 mm. To use the Zwick tensile testing machine to carry out the tensile test along the rolling direction, use the small load Vickers hardness tester HV-5SPTA and the cupping test machine BCS50A to carry out the Vickers hardness test and Erichsen cupping test, the load is 500gf, and the pressure is maintained for 15s. The bending angle is detected on an electronic universal testing machine, and the sample size is 60 × 60 mm.

3 Result and discussion

Hot rolling is a complex heat-activated process. To obtain the expected surface quality and mechanical properties of hot-stamped steel, it is necessary to strictly control the hot-rolling temperature and hot-rolling conditions to obtain uniform ferrite and pearlite structures (Du et al., 2022; Du et al., 2023b). It can be seen from Figure 3 that the processing technology we designed can obtain hot-rolled samples with uniform microstructure. Using the statistics of Image Pro software, it can be seen that the hot-rolled sample is composed of ~76% volume fraction of ferrite with irregular grain boundaries and ~24% volume fraction of lamellar pearlite. After blasting, the surface quality of the hot-rolled samples can meet the conditions of cold-rolling (Figure 1). Under the rolling force of cold rolling, the microstructure of the hot-rolled samples undergoes severe plastic deformation along the rolling direction, and even after short-term continuous annealing, the strip-like characteristics are still retained. Ferrite is elongated and refined during cold rolling and annealing. Pearlite was precipitated during annealing, and the content increased to 31%. After the annealed sample is quenched by a flat die, a uniform microstructure of equiaxed ferrite, martensite, and a small amount of acicular bainite is obtained. The ferrite content is reduced to ~62%, and the volume fraction of martensite and bainite is ~38%.

During the process of hot rolling, cold rolling, annealing, and flat die quenching, the strength of the experimental sample fluctuates slightly. The yield strength of the hot rolled sample is 606MPa, the tensile strength is 667MPa, and the elongation is 11.06% (Figure 4). During the cold rolling process of hot-rolled

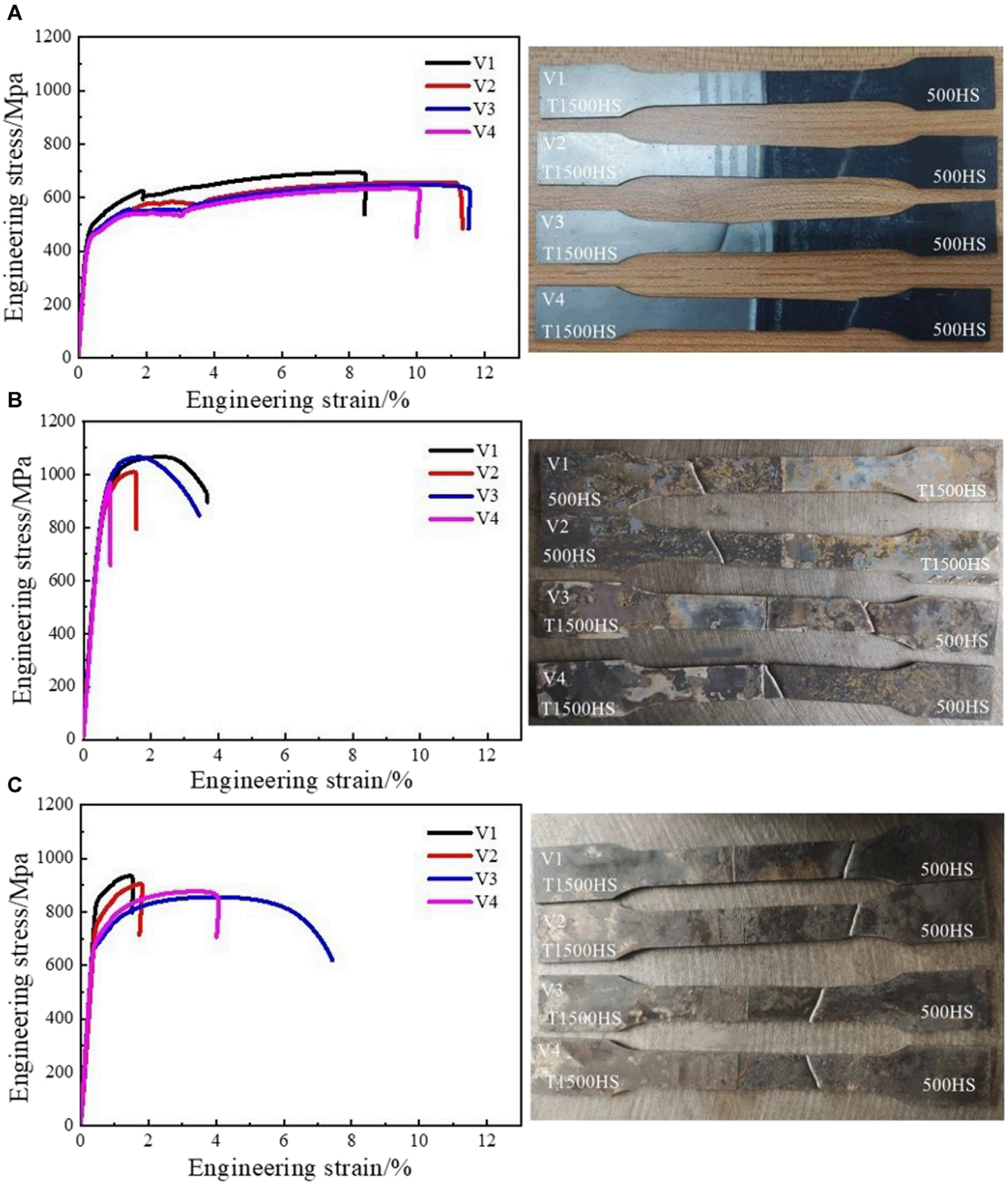

FIGURE 7
Engineering stress-strain curves and post-fracture states of soft/hard composite samples prepared by a laser welding technique, **(A)** annealed sample, **(B)** quenched sample, **(C)** quenched and tempered sample.

samples, ferrite grain refinement and lamellar pearlite fragmentation are induced, resulting in higher grain boundary strengthening. It can be predicted that this process will inevitably increase the strength. According to the law of strength-plasticity inversion of metal materials (Du et al., 2023a), due to the introduction of substructures and the accumulation of distortion energy, the plasticity of materials is bound to be deteriorated. In order to match the strength and plasticity of the material, the migration of

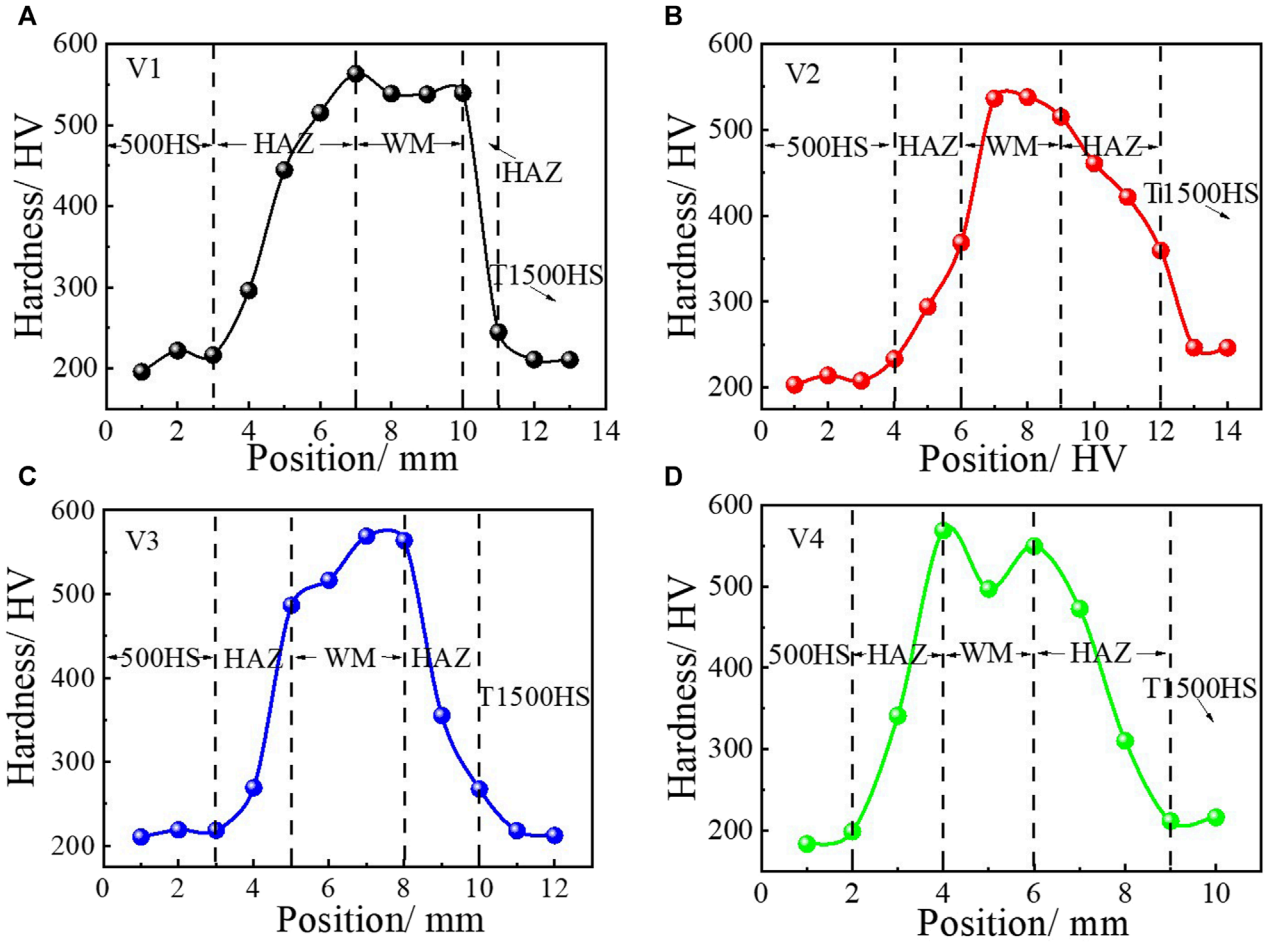

FIGURE 8
Weld hardness distribution before heat treatment, **(A)** V1, **(B)** V2, **(C)** V3, **(D)** V4.

grain boundaries and the merging of dislocations are controlled by cold rolling and continuous annealing, and higher grain boundary strengthening and dislocation strengthening are introduced into the microstructure so that the strength of the sample varies less, it also has higher plasticity. The yield strength of the annealed sample after cold rolling was 580 MPa, the tensile strength was 632 MPa, and the elongation was 13.1% (Figure 4). The annealed samples after cold rolling were austenitized and die-quenched to introduce a small amount of hard martensitic microstructure, allowing the material to continue to maintain deformation resistance (Figure 4). The strength of the flat die quenched sample decreased slightly, the yield strength was 492MPa, the tensile strength was 644MPa, the elongation was 13.67%, and the bending angle reached 150° (Figure 4A). The full-process hot stamping 500HS we designed has excellent comprehensive mechanical properties (Figure 4B), has broad industrialization prospects, and provides the basis for the subsequent preparation of soft/hard composite automotive steel.

The hard T1500HS sample and the soft 500HS sample developed are used as the base material, and the two are combined by laser welding technology to explore the microscopic morphology and deformation characteristics of the weld. There are significant differences in the chemical composition and phase transition points of the two base metals, which make the parts of the joints of the samples heated unevenly during the welding thermal cycle, resulting in differences in the microstructure and width of each area. The width of the heat-affected zone of T1500HS is larger than 500HS. It is found in Figure 4 that the welding speed of V1 and V2 samples is relatively slow, the amount of molten metal is relatively large, and the surface tension is difficult to maintain the molten pool in the weld, but sinks from the middle of the weld, forming pits, and the sinking phenomenon occurs (Figures 5A1, B1). The weld seam of the V3 sample is flat, the microstructure is fine and dense, and there is no obvious boundary (Figure $5C_1$). Due to the faster welding speed of the V4 sample, the liquid metal flowing in the center of the weld had no time to redistribute, so it solidified on both sides of the weld, forming undercut defects (Figure $5D_1$).

As shown in Figure 5, it can be seen that the weld area under each process is composed of martensitic microstructure. It is because the heat of the laser beam is concentrated during the welding process, causing the peak temperature of the weld area to reach the melting point temperature of the base metal, which quickly makes the base metal on both sides Melt and fuse with each other, and the welding heat diffuses to the base metal on both

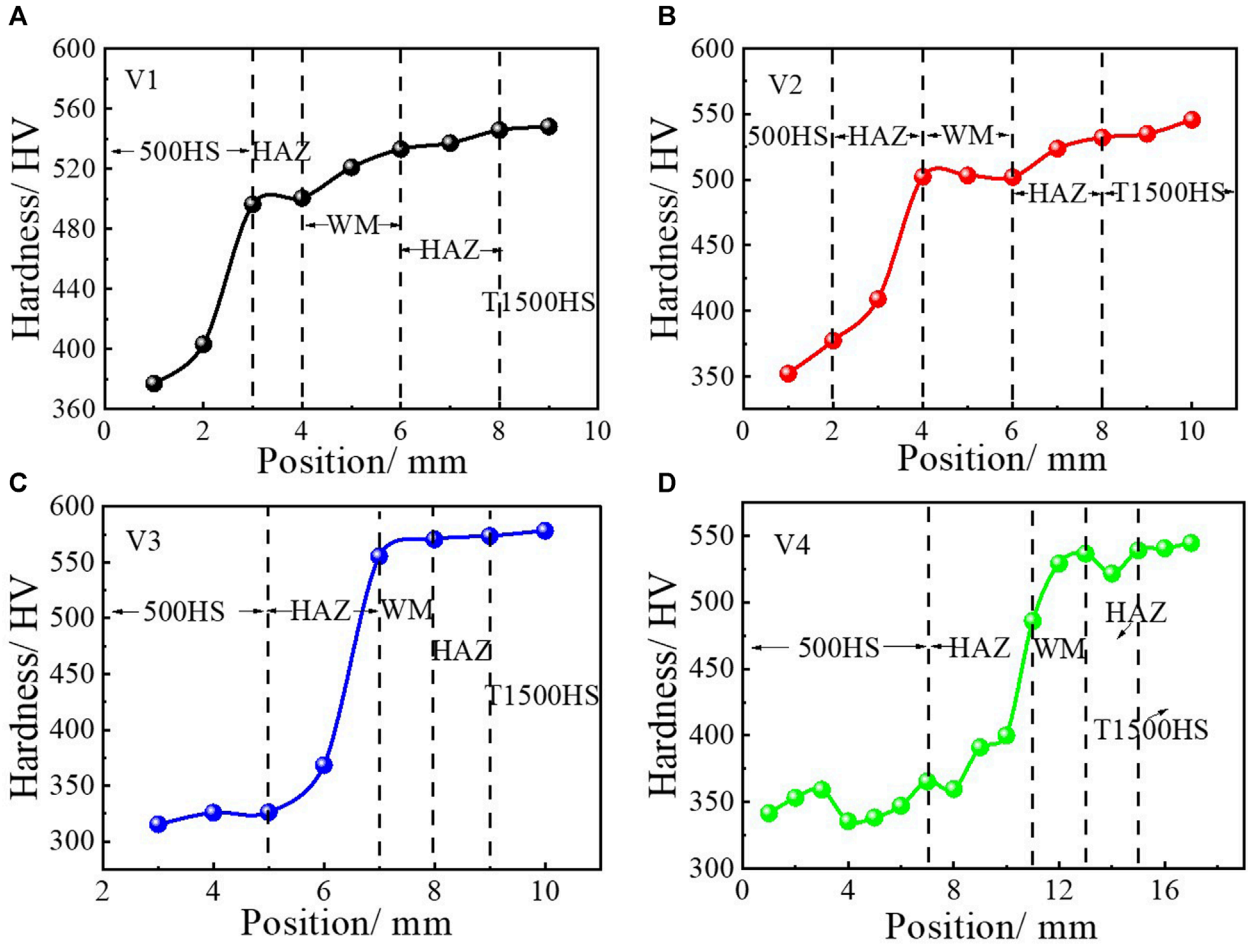

FIGURE 9
Weld hardness distribution after heat treatment, **(A)** V1, **(B)** V2, **(C)** V3, **(D)** V4.

sides, the weld zone has a faster heating rate and cooling rate, and martensite structure is formed during the rapid cooling process. Each sample has the same feature, and the microstructure of lath martensite in the heat-affected zone of T1500HS is more obvious (Figure 5). Due to the high temperature obtained in this area and the large span, the base metal is partially austenitized. During the subsequent cooling process, ferrite and martensite are formed in the heat-affected zone near the weld, and there are still Pearlite organization. The microstructure of the 500HS heat-affected zone on the other side (Figures $5A_4$–D_4), which is similar to the T1500HS side, is martensite and ferrite and contains a small amount of granular bainite. With the increase of welding speed, the content of martensite in the structure increases obviously, and the content of granular bainite decreases. The difference in the structure of the heat-affected zone on both sides of the welded joint is mainly due to the difference in the chemical composition of the base metal on both sides. T1500HS has added part of Cr, and the high-temperature austenite is relatively stable. During the cooling process of the sample during welding, due to its good hardenability, a large amount of martensite microstructure will be formed in the weld. The 500HS contains relatively fewer carbon and alloy elements, and the critical cooling rate for obtaining martensite is relatively high. During the welding cooling process, pearlite and bainite structures are easily formed.

After the weld martensite is heated, the microstructure of the weld undergoes static recrystallization. During the quenching and cooling process, the columnar crystals disappear and are replaced by relatively regular equiaxed crystals, showing a non-directional lath martensite. Body and the structure is denser than before quenching. As can be seen in Figure 6, after quenching and tempering at a low temperature of 170°C, a clear martensitic microstructure can still be observed.

The engineering stress-strain curves and related comprehensive mechanical properties of each welded sample are shown in Table 2 and Figure 7. After laser welding, the strength of tailor-welded blank samples under the four welding processes is between the two base metals (500HS and T1500HS). There is a burning loss of the total elements during the welding process, and the elements redistribute after welding. The alloy composition of the material varies greatly, and the alloy elements of the joint change under the action of the welding heat cycle (Yu et al., 2023). After cooling, the weld zone has higher strength and hardness. During the stretching process, the deformation will be concentrated on the base metal on both sides, while the deformation of the welded joint in the middle of the sample

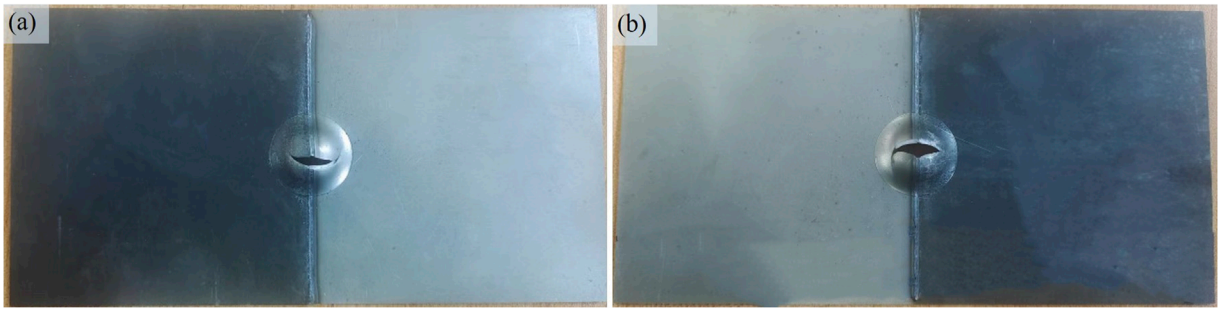

FIGURE 10
Cupping test of V3 sample before and after heat treatment: **(A)** before heat treatment; **(B)** after heat treatment.

is very small, which increases the deformation inhomogeneity of the entire sample, and eventually causes the sample to break at the base metal. In comparison, the comprehensive mechanical properties of V3 are better. It shows that the welding speed is an important factor affecting the welding quality. If the welding speed is too low, the material will vaporize, while if the welding speed is too high, the weld will not penetrate and the performance of the joint will deteriorate (Chaudry et al., 2023).

It can be seen from Table 2 and Figure 7 that after heat treatment of laser welded blanks, V3 still has high comprehensive mechanical properties, its fracture strength is moderate, and the fracture positions are all located at 500HS. It is considered that it is mainly caused by the large difference in strength between T1500HS and 500HS base metal after quenching. During the stretching process, the weaker base metal 500HS deformed first. Due to the higher strength of the weld, the weld did not reach yield during the stretching process, and the 500HS had already necked and finally fractured. After tempering treatment, V3 still has better overall performance, its fracture strength decreases slightly, and its strength is higher than that of the lower base material 500HS, and its elongation increases. It can be seen that the process meets the welding requirements of 500HS and T1500HS. During the stress process, the weld deviates to the high-strength T1500HS side, and stress concentration occurs on the low-strength 500HS side. After quenching and subsequent tempering, the weld still maintains high strength, the tensile specimen necks and breaks at the low-strength 500HS side, and the weld meets the service requirements.

The hardness distribution of tailor-made welded blanks before heat treatment is shown in Figure 8. The hardness of the four processes all showed a trend of increasing first and then decreasing, that is, the base metal T1500HS < heat-affected zone (HAZ) < weld (WM) < HAZ < base metal 500HS. The peak of hardness distribution is located in the weld zone. This is due to the small heat of laser welding and the fast cooling rate during welding, which exceeds the critical cooling rate of martensite transformation, and the microstructure is all martensite. The hardness value of the base metal area is the lowest, and compared with the peak value of the weld area, the hardness difference between the two is as high as 386HV. The heat-affected zone near the weld is ferrite and martensite (Figure 5), while pearlite and bainite exist on the side near the base metal, and the hardness tends to be low on both sides and high in the middle. Overall, the difference in hardness between the weld and the base metal at the four welding speeds is basically the same.

The hardness of the weld after quenching was detected and analyzed. As shown in Figure 9, under the four-speed processes, the hardness increases monotonously from the 500HS side of the base metal to the T1500HS side, and the hardness distribution peak is located on the T1500HS base metal side. This is because T1500HS is completely transformed into quenched martensite after high-temperature quenching, and 500HS is transformed into ferrite and martensite microstructure, while the microstructure of the weld zone hardly changes, and the maximum hardness difference reaches 205HV.

The welding quality of laser overlaid plates was examined by conducting a cupping test using a plate forming machine, as shown in Figure 10. The cupping cracks formed perpendicular to the weld, without tearing along the weld, which verifies the feasibility of laser welding technology for composite joining of soft steel and hard steel, with good weld quality. Normally, a higher content of martensite in the weld can enhance hardness and strength but may deteriorate ductility to some extent. However, the higher content of bainite and pearlite in the heat-affected zone enables the adaptation and transmission of external loads during the cupping process, thereby improving the weld's plasticity and ductility.

4 Conclusion

This work designs a 500 MPa grade hot stamping 500HS composed of a large amount of ferrite and a small amount of martensite. The annealed sample is subjected to plane quenching treatment, and its mechanical properties show the same law as that of the annealed sample, reaching the industry standard, achieving 150° bending without cracking, and showing a wide range of industrialization prospects.

The preparation of 500 MPa grade soft/hard composite hot stamping steel is realized here. The changes in microstructure, mechanical properties, and microhardness before and after tailor welding and heat treatment of 500HS and T1500HS at different laser speeds were studied. We found that before heat treatment, the comprehensive mechanical properties of laser-welded blanks

at four welding speeds were between the two base metals. Before heat treatment, the welds under different processes can all be transformed into martensite. However, due to the different alloy composition, the heat-affected zone on the T1500HS side is basically completely transformed into martensite, while the 500HS side still has part of bainite and Pearlite. The hardness peak of tailor-welded joints is located in the weld zone. After heat treatment, the weld structure is still all martensitic, but denser than before. The weld seam shifts to the high-strength T1500HS side and stress concentration occurs on the low-strength 500HS side, and the weld seam still maintains a high strength. The hardness of the weld joint increases monotonically from the 500HS side to the T1500HS side. The comprehensive mechanical properties obtained at the welding speed of 3.5 m/min are the best, and the loss of comprehensive properties caused by the weld seam is the smallest.

Data availability statement

The original contributions presented in the study are included in the article/supplementary material, further inquiries can be directed to the corresponding authors.

Author contributions

YY: Data curation, Formal Analysis, Investigation, Methodology, Validation, Writing–original draft. ZW: Data curation, Project administration, Supervision, Validation, Visualization, Writing–review and editing. BC: Data curation, Formal Analysis, Investigation, Validation, Visualization, Writing–review and editing. SZ: Formal Analysis, Writing–review and editing. JD: Conceptualization, Resources, Writing–review and editing.

Funding

The author(s) declare financial support was received for the research, authorship, and/or publication of this article. This research was supported by the Jiangsu Key Laboratory of Asic Design (Wuxi) (No. 2021KLOP007) and Key Research Project of Jiangsu Vocational College of Information Technology (JSITKY202202).

Acknowledgments

Experimental equipment and technical support of China Shougang Jingtang Company, Tangshan Iron and Steel Company Technology Center, and North China University of Science and Technology.

Conflict of interest

Authors YY and BC were employed by Shougang Group, Shougang Jingtang United Iron and Steel Co., Ltd. Author ZW was employed by Tangshan Iron and Steel Group Co., Ltd.

The remaining authors declare that the research was conducted in the absence of any commercial or financial relationships that could be construed as a potential conflict of interest.

Publisher's note

References

Bhargava, M., Chakrabarty, S., Barnwal, V. K., Tewari, A., and Mishra, S. K. (2018). Effect of microstructure evolution during plastic deformation on the formability of transformation induced plasticity and quenched & partitioned AHSS. *Mater. Des.* 152, 65–77. doi:10.1016/j.matdes.2018.04.068

Cann, J. L., De Luca, A., Dunand, D. C., Dye, D., Miracle, D. B., Oh, H. S., et al. (2021). Sustainability through alloy design: challenges and opportunities. *Prog. Mater. Sci.* 117, 100722. doi:10.1016/j.pmatsci.2020.100722

Chaudry, U. M., Han, S.-C., and Jun, T.-S. (2023). Effect of welding speed on the microstructure and texture development in the individual weld zone of friction stir welded DP780 steel. *J. Mater. Res. Technol.* 23, 4976–4989. doi:10.1016/j.jmrt.2023.02.122

Chen, X., Inao, D., Li, X., Tanaka, S., Li, K., and Hokamoto, K. (2022). Optimal parameters for the explosive welding of TP 270C pure titanium and SUS 821L1 duplex stainless steel. *J. Mater. Res. Technol.* 19, 4771–4786. doi:10.1016/j.jmrt.2022.07.031

Costa, P., Altamirano-Guerrero, G., Salinas-Rodríguez, A., Salas-Reyes, A. E., and Goodwin, F. (2022). Dilatometric study of continuous cooling transformation of intercritical austenite in cold rolled AHSS-DP steels. *J. Mater. Res. Technol.* 19, 4360–4370. doi:10.1016/j.jmrt.2022.06.140

Dong, W., Lei, M., Pan, H., Ding, K., and Gao, Y. (2022). Role of the internal oxidation layer in the liquid metal embrittlement during the resistance spot welding of the Zn-coated advanced high strength steel. *J. Mater. Res. Technol.* 21, 3313–3326. doi:10.1016/j.jmrt.2022.10.154

Drexler, A., Bergmann, C., Manke, G., Kokotin, V., Mraczek, K., Pohl, M., et al. (2021). On the local evaluation of the hydrogen susceptibility of cold-formed and heat treated advanced high strength steel (AHSS) sheets. *Mater. Sci. Eng. A* 800, 140276. doi:10.1016/j.msea.2020.140276

Du, J., Li, J., Feng, Y., Li, Y., and Zhang, F. (2023a). Exploring nonlinear strengthening in polycrystalline metallic materials by machine learning methods and heterostructure design. *Int. J. Plast.* 164, 103587. doi:10.1016/j.ijplas.2023.103587

Du, J., Li, J., Feng, Y., Ning, J., Liu, S., and Zhang, F. (2022). Effect of layered heterogeneous microstructure design on the mechanical behavior of medium carbon steel. *Mater. Des.* 221, 110953. doi:10.1016/j.matdes.2022.110953

Du, J., Liu, G., Feng, Y., Feng, H., Li, T., and Zhang, F. (2023b). Strength and ductility enhancement of plain carbon steel by heterostructure design. *Mater. Sci. Eng. A* 868, 144770. doi:10.1016/j.msea.2023.144770

Du, J. L., Feng, Y. L., and Zhang, M. (2021). Construction of a machine-learning-based prediction model for mechanical properties of ultra-fine-grained Fe–C alloy. *J. Mater. Res. Technol.* 15, 4914–4930. doi:10.1016/j.jmrt.2021.10.111

Feistle, M., Golle, R., and Volk, W. (2022). Edge crack test methods for AHSS steel grades: a review and comparisons. *J. Mater. Process. Technol.* 302, 117488. doi:10.1016/j.jmatprotec.2021.117488

Hong, M., Wang, S., Sun, W., Geng, Z., Xin, J., and Ke, L. (2022). Effect of welding speed on microstructure and mechanical properties of selective laser melting Inconel 625 alloy laser welded joint. *J. Mater. Res. Technol.* 19, 2093–2103. doi:10.1016/j.jmrt.2022.06.020

Hu, B., Luo, H., Yang, F., and Dong, H. (2017). Recent progress in medium-Mn steels made with new designing strategies, a review. *J. Mater. Sci. Technol.* 33, 1457–1464. doi:10.1016/j.jmst.2017.06.017

Lai, Z.-H., Lin, Y.-T., Sun, Y.-H., Tu, J.-F., and Yen, H.-W. (2022). Hydrogen-induced ductilization in a novel austenitic lightweight TWIP steel. *Scr. Mater.* 213, 114629. doi:10.1016/j.scriptamat.2022.114629

Li, Y., Liang, Z., Zhang, Z., Zou, T., Li, D., Ding, S., et al. (2019). An analytical model for rapid prediction and compensation of springback for chain-die forming of an AHSS U-channel. *Int. J. Mech. Sci.* 159, 195–212. doi:10.1016/j.ijmecsci.2019.05.046

Liang, Z., Liu, Y., Zou, T., Li, D., Ding, S., Xiao, H., et al. (2021). Analysis and suppression of flange wrinkling in AHSS chain-die forming channels with a curved axis. *J. Manuf. Process.* 71, 70–84. doi:10.1016/j.jmapro.2021.09.006

Manladan, S. M., Jang, Y., and Park, Y.-D. (2023). Effect of paint baking on the halo ring and mechanical behavior of 30MnB5 hot-stamped steel resistance spot welding joints. *J. Mater. Res. Technol.* 24, 4756–4761. doi:10.1016/j.jmrt.2023.04.144

Razmpoosh, M. H., DiGiovanni, C., Zhou, Y. N., and Biro, E. (2021). Pathway to understand liquid metal embrittlement (LME) in Fe-Zn couple: from fundamentals toward application. *Prog. Mater. Sci.* 121, 100798. doi:10.1016/j.pmatsci.2021.100798

Šebestová, H., Horník, P., Mrňa, L., and Doležal, P. (2018). Microstructure and mechanical properties of hybrid LasTIG welds of HSLA steel. *10th CIRP Conf. Photonic Technol. LANE* 74, 743–747. doi:10.1016/j.procir.2018.08.019

Sedaghat-Nejad, R., Shahverdi, H. R., and Askari-Paykani, M. (2022). Introduction and mechanical evaluation of a novel 3rd-generation medium manganese AHSS with 86 GPa% of PSE. *Mater. Sci. Eng. A* 843, 143104. doi:10.1016/j.msea.2022.143104

Soleimani, M., Kalhor, A., and Mirzadeh, H. (2020). Transformation-induced plasticity (TRIP) in advanced steels: a review. *Mater. Sci. Eng. A* 795, 140023. doi:10.1016/j.msea.2020.140023

Sun, W. W., Wu, Y. X., Yang, S. C., and Hutchinson, C. R. (2018). Advanced high strength steel (AHSS) development through chemical patterning of austenite. *Scr. Mater.* 146, 60–63. doi:10.1016/j.scriptamat.2017.11.007

Xu, W., Tao, W., Luo, H., and Yang, S. (2023). Effect of oscillation frequency on the mechanical properties and failure behaviors of laser beam welded 22MnB5 weld. *J. Mater. Res. Technol.* 22, 1436–1448. doi:10.1016/j.jmrt.2022.12.013

Yu, D., Zhang, Y., Hosseini, S. R. E., Zhou, J., and Sun, D. (2023). Element diffusion and microstructure evolution at interface of stainless steel/Ti alloy joint by laser welding with AgCuTi filler metal. *J. Mater. Res. Technol.* 24, 6463–6472. doi:10.1016/j.jmrt.2023.04.217

Yu, S., Long, M., Zhang, M., Chen, D., Xu, P., Duan, H., et al. (2021). Effect of mold corner structures on the fluid flow, heat transfer and inclusion motion in slab continuous casting molds. *J. Manuf. Process.* 68, 1784–1802. doi:10.1016/j.jmapro.2021.06.067

Zhang, M., Wan, Z., and Li, L. (2015). Transformation characteristics and properties of B steel 22MnB5. *Int. Conf. Martensitic Transform. ICOMAT-2014* 2, S697–S700. doi:10.1016/j.matpr.2015.07.378

Zhang, S., Li, J., Peng, Z., Liu, S., Huang, F., and Liu, J. (2023). Synergistic effects of Ta and Mo on the hydrogen embrittlement resistance in ultra-high strength hot stamping steel. *Mater. Sci. Eng. A* 872, 144956. doi:10.1016/j.msea.2023.144956

Zhang, W., and Xu, J. (2022). Advanced lightweight materials for Automobiles: a review. *Mater. Des.* 221, 110994. doi:10.1016/j.matdes.2022.110994

Zhao, Y., Yang, D., Qin, Z., Chu, X., Liu, J., and Zhao, Z. (2022). A novel hot stamping steel with superior mechanical properties and antioxidant properties. *J. Mater. Res. Technol.* 21, 1944–1959. doi:10.1016/j.jmrt.2022.10.017